Inelastic response spectra for seismic design verification of pipe and stiffened box steel bridge piers

Qingyun Liu*, Akira Kasai**, Tsutomu Usami***

* Dr. of Eng., (Former Graduate Student, Dept. of Civil Eng., Nagoya University, Chikusa-ku, Nagoya 464-8603)
** M. of Eng., Research Associate, Dept. of Civil Eng., Nagoya University, Chikusa-ku, Nagoya 464-8603
*** Dr. of Eng., Dr. of Sc., Professor, Dept. of Civil Eng., Nagoya University, Chikusa-ku, Nagoya 464-8603

Currently, inelastic seismic design verification of hollow steel bridge piers depends on direct time history analysis to estimate seismic demand in case of a severe earthquake. This paper proposes inelastic response spectra for simple and quick design verification without time history analysis. Example spectra are plotted for pipe-section and stiffened box-section steel bridge piers based on an accurate SDOF hysteretic model—the damage-based hysteretic model. Since the proposed spectra directly reflect demand versus capacity, examining these example spectra helps gain valuable insights into the relation between ductility capacity of the structure and its safety margin against severe earthquakes.

Key words :response spectra, hysteretic model, seismic, steel bridge piers

1. Introduction

The current Design Specifications of Highway Bridges of Japan Road Association[1] (the JRA code) follows a dual-criteria strategy in the seismic design of thin-walled steel bridge piers: The structure must be designed to respond elastically to a moderate earthquake which is highly likely to occur in its life span; On the other hand, in case of a severe earthquake, the structure is allowed to undergo some inelastic deformation but not collapse. The dual-criteria strategy leads to a two-phase design procedure: a preliminary elastic seismic design stage corresponding to moderate earthquake conditions and ultimate limit state design stage to severe earthquake conditions.

Because of their important position in the urban transportation system, it is preferable that highway bridges do not lose their main function even after a severe earthquake. The ultimate limit state design philosophy now does not settle for merely preventing collapse but seek to limit damage so that highway bridges can resume normal functioning as quickly as possible after a major earthquake. Thus the definition of ultimate limit state for steel bridge piers should limit the seismic damage to an acceptable degree. And the current JRA code[1] suggests that dynamic analysis be carried out using the prescribed Level 2 design accelerograms to check that maximum displacement and residual displacement do not exceed structural capacity.

Since direct time history analysis is quite inconvenient in practical design, this study proposes the use of inelastic response spectra to circumvent the relatively complicated dynamic analysis procedure and enable simple and quick ultimate limit state verification of centrally loaded steel bridge piers. An accurate hysteretic model — the damage-based hysteretic model[2)~5)] is used to plot the maximum displacement spectra and residual displacement spectra for several pipe and stiffened box cross sections. The trends of demand versus capacity reflected in these spectra shed new lights on the relation between ductility capacity of the structure and its safety margin against severe earthquakes. Right after this introduction is a brief review of the damage-based hysteretic model. Next, concepts and analysis procedure used for generating the inelastic spectra are treated. Then the example spectra based on the damage-based hysteretic model are presented. Finally, the results obtained in these spectra are discussed and summarized in conclusion.

2. Review of Damage-based Hysteretic Model[2)~5)]

2.1 Damage index formulation[2)~3)]

The damage-based model is an accurate hysteretic model developed for thin-walled steel bridge piers of pipe section or box section. The damage-based hysteretic model centers around a comprehensive damage index. The damage index is a global index to quantify damage due to coupled local buckling and global instability under the combined action of a constant vertical load and cyclic lateral loading. The damage index D for thin-walled steel bridge piers is defined as[3]:

$$D=(1-\beta)\sum_{j=1}^{N_1}\left[\left(\frac{\delta_{max,j}-\delta_y}{\delta_u-\delta_y}\right)^c\right]+\beta\sum_{i=1}^{N}\left[\left(\frac{E_i}{0.5(H_y+H_{max,1})(\delta_u-\delta_y)}\right)^c\right] \quad (1)$$

The first term of Eq.(1) accounts for damage due to large inelastic deformation, and the second term for damage due to hysteretic energy. H_y and δ_y are yield horizontal load and yield horizontal displacement respectively; δ_u is the displacement at collapse under monotonic loading; $\delta_{max,j}$ is maximum absolute displacement for the j-th half-cycle; N_1 is the number of half-cycles producing $\delta_{max,j}$ such

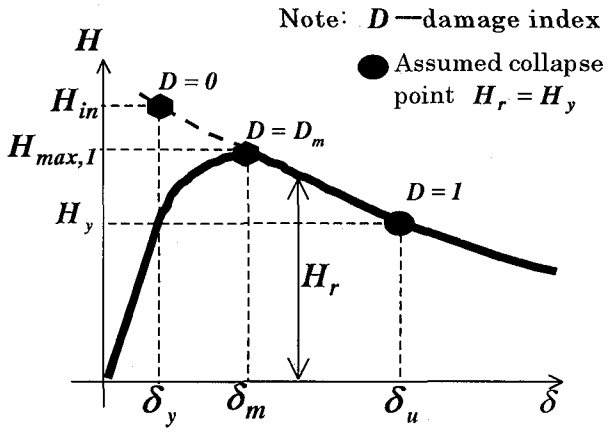

Fig. 1 Degradation of strength (monotonic loading)

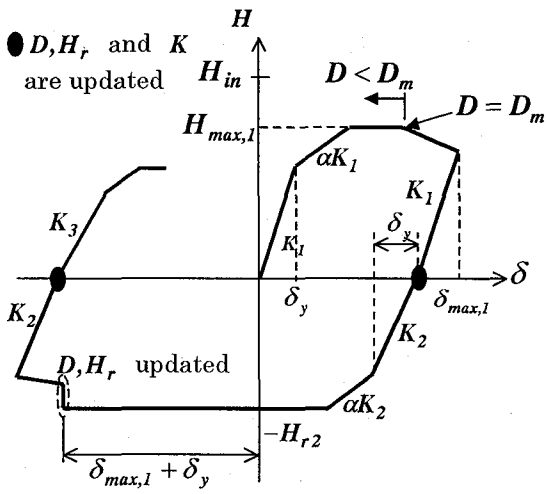

Note: K_2, K_3 **are calculated values of** K **by Eq.(3).**

Fig. 2 Damage-based hysteretic model

that $\delta_{max,j} > \delta_{max,j-1} + \delta_y$ and the initial reference $\delta_{max,0}$ is designated as δ_y; E_i is the hysteretic energy absorbed during the *i-th* half-cycle; The quantity used to normalize E_i — $0.5(H_y + H_{max,1})(\delta_u - \delta_y)$ is an estimation of dissipated energy up to collapse under monotonic loading, in which $H_{max,1}$ stands for peak strength under monotonic loading. There are two free parameters in the damage index expression— β and c. β is to specify the relative importance of deformation-based damage and hysteretic energy-based damage. Parameter c has two major functions: firstly, $c > 1.0$ gives relatively more importance to larger half-cycles; on the other hand, since it is the power to contribution from every half cycle (normalized half-cycle deformation and normalized half-cycle hysteretic energy), it serves to relate damage under general cyclic condition to damage under simple monotonic condition.

Collapse state is defined as when the residual strength H_r (strength on the descending branch) drops to H_y (See **Fig.1**)[2)-3)]. By normalizing the deformation term and the plastic energy term in the damage index formulation, it is intended that the damage index always come to unity at collapse under general cyclic loading; Parameter β and c for either pipe-section steel bridge piers or box-section steel bridge piers are determined based on this criterion[3)].

2.2 Damage-based hysteretic model[2)-5)]

The damage index forms the basis of the damage-based hysteretic model in that degradation of strength and stiffness is prescribed as depending solely on damage index[2)]:

$$H_r = H_{in} \cdot \left(\frac{H_y}{H_{in}}\right)^D \tag{2}$$

$$K = K_1 \cdot \left(\frac{H_y}{H_{in}}\right)^D \tag{3}$$

where D denotes the damage index; K_1 is the initial elastic stiffness; H_{in} is the imaginary strength at $D = 0$. **Fig.1**[3)] illustrates strength degradation process from the initial state of $H_r = H_{in}$ to collapse point of $H_r = H_y$ under monotonic loading. Calculation of parameter H_{in} is detailed in Ref. 3; it largely depends on peak monotonic strength $H_{max,1}$.

The hysteretic model is of piecewise multi-linear type. Basically the loading branch follows a trilinear skeleton of an elastic limb, a hardening limb and a perfectly plastic limb. With updating of the damage index and residual strength, there may also be a descending limb in addition to the above three limbs. **Fig.2** illustrates the loading and unloading rules of this model[5)]. The parameter α defines the ratio of hardening stiffness to elastic stiffness, and can be extracted from the monotonic $H - \delta$ curve[4)]. The damage index D is calculated throughout loading history; At any point, the current residual strength and unloading stiffness are determined according to current damage index value.

2.3 Model parameters[3)-5)]

Model parameters are summarized as follows:

(1) Free parameters in the damage index — β and c;

(2) δ_u, $H_{max,1}$, δ_m and α; these parameters are to be extracted from the monotonic $H - \delta$ curve.

It can be seen that all the parameters needed in the damage-based hysteretic model are derived from monotonic $H - \delta$ behavior except for β and c. It is through β and c that the model is able to predict hysteretic behavior under general cyclic loading based on the few major monotonic characteristics.

To facilitate practical application, all the model parameters have been expressed in terms of structural parameters of pipe-section or stiffened box-section steel bridge piers.

2.3.1 Model parameters for pipe steel bridge piers

For pipe section steel bridge piers, β and c are given by[3)]:

$$\beta = 0.27 \tag{4}$$

$$c = 1.69\bar{\lambda} + 0.93 \quad (0.20 \le \bar{\lambda} \le 0.50) \tag{5}$$

Monotonic model parameters for pipe-section steel bridge piers can be calculated from the following empirical equations[3)]:

Table 1 Ranking of damage degree[7]

Rank	Residual Displacement	Damage Degree
No damage	$\delta_R < h/1000$	Almost no damage
Small damage	$h/1000 \le \delta_R < h/300$	Several days needed for repairing. Passable to ordinary vehicles while being repaired
Medium damage	$h/300 \le \delta_R < h/150$	Passable only to emergency vehicles. Two weeks to two months needed for repairing
Severe damage	$h/150 \le \delta_R < h/100$	Not collapsed, but have lost function. More than two months needed for repairing
Collapse	$\delta_R \ge h/100$	Collapsed

Note: δ_R — residual displacement; h — pier height.

$$\frac{H_{max,1}}{H_y} = \frac{\left[0.204(1+P/P_y)\right]^{4.87}}{(R_t^2\bar{\lambda})^{0.8}} + 1.32 \quad (6)$$

$$\frac{\delta_m}{\delta_y} = \frac{0.00064}{\left(R_t\sqrt{\bar{\lambda}}\right)^{2.61}} + 1.04 \quad (7)$$

$$\frac{\delta_u}{\delta_y} = \frac{0.037}{(1+P/P_y)^{2.5} R_t^{1.89}\bar{\lambda}^{1.14}} + 1.15 \quad (8)$$

$$\alpha = \left(\frac{0.081}{R_t}\right)^{3.93} \bar{\lambda}^{0.01R_t^{-2}} + 6.3R_t - 0.1 \quad (9)$$

In Eqs.(4)~(9), R_t =radius-thickness ratio parameter, $\bar{\lambda}$ =slenderness ratio parameter, and P/P_y =axial load ratio (P_y =squash load of the cross section). Definitions of R_t and $\bar{\lambda}$ are given in Appendix.

2.3.2 Model parameters for stiffened box steel bridge piers

For stiffened box-section steel bridge piers (stiffness ratio of longitudinal stiffeners $\gamma/\gamma^* \ge 3$), β and c are determined as[5]:

$$\beta = 0.11 \quad (10)$$

$$c = 1.96\bar{\lambda} + 1.12 \quad (0.20 \le \bar{\lambda} \le 0.50) \quad (11)$$

And monotonic parameters for the corresponding box-section steel bridge piers can be calculated by[5]:

$$\frac{H_{max,1}}{H_y} = \frac{0.33(1+P/P_y)^{0.8}}{\left(R_f^{1.5}\bar{\lambda}\sqrt{\bar{\lambda}_s'}\right)^{0.27}} + 0.64 \quad (12)$$

$$\frac{\delta_m}{\delta_y} = \frac{0.95}{\left(\sqrt{R_f}\,\bar{\lambda}\,\bar{\lambda}_s'^{\,5}\right)^{0.33}} - 6.47 \quad (13)$$

$$\frac{\delta_u}{\delta_y} = \frac{0.76}{(1+P/P_y)^2 \cdot \left(\sqrt{R_f}\,\bar{\lambda}\,\bar{\lambda}_s'\right)^{1.3}} - 1.46 \quad (14)$$

$$\alpha = 0.3 \quad (15)$$

In Eqs.(10)~(15), R_f =width-thickness ratio parameter of the flange plate, $\bar{\lambda}_s'$ =modified stiffener's equivalent slenderness ratio parameter, and is defined by[6]:

$$\bar{\lambda}_s' = \bar{\lambda}_s / \sqrt[3]{\bar{\alpha}} \quad (16)$$

wherein $\bar{\lambda}_s$ = stiffener's equivalent slenderness ratio parameter, $\bar{\alpha}$ =aspect ratio of flange panel between two diaphragms. Definitions of R_f and $\bar{\lambda}_s$ can be found in Appendix.

3. Evaluation of Structure Capacity

The current JRA code[1] requires the check of maximum displacement and residual displacement in the ultimate limit state design stage. To prohibit excessive maximum displacement, the current JRA code[1] suggests the allowable maximum displacement be the value at cyclic strength peak or a value corresponding to a small degree of strength degradation under static cyclic loading. In this study, allowable maximum displacement is chosen as δ_{95} —the displacement value that corresponds to the cyclic strength (under reversed static cyclic loading) dropping to 95% of the peak cyclic strength. Based on cyclic FEM analysis that takes into account local and overall interaction buckling, empirical equations of δ_{95} for both box-section and pipe-section steel bridge piers are obtained[6]. **For pipe-section steel bridge piers,**

$$\frac{\delta_{95}}{\delta_y} = \frac{0.24}{(1+P/P_y)^{2/3} R_t \bar{\lambda}} \quad (17)$$

And **for stiffened box-section steel bridge piers,**

$$\frac{\delta_{95}}{\delta_y} = \frac{0.25}{(1+P/P_y) R_f \sqrt{\bar{\lambda}\,\bar{\lambda}_s'}} + 2.31 \quad (18)$$

Eqs.(17) and (18) are adopted for evaluation of structural capacity in the inelastic response spectra presented in **Section 5** and **Section 6**.

As to the allowable residual displacement, $0.01h$ is deemed as the repairable limit after a severe earthquake according to the JRA code[1], wherein h stands for pier height. Ref. 7 divides damage degree of steel bridge piers into five ranks based on residual displacement δ_R and the corresponding time needed for repair (**Table 1**), and suggests that for important highway bridges, allowable residual displacement be set smaller than $0.01h$. Besides $0.01h$, two additional yardsticks from **Table 1** — $h/150$ and $h/300$ are also marked out in the residual displacement spectra.

4. Analysis Procedure

The equation of motion for the SDOF system modeling steel bridge piers can be written as:

$$\ddot{u} + 2\xi\omega \cdot \dot{u} + H / M = -\ddot{u}_g \tag{19}$$

where M, ξ, H, ω are the mass, damping ratio, the restoring force and natural frequency respectively. Damping ratio is taken as 0.05. The relationship between restoring force H and displacement u shall be prescribed by a hysteretic model. And major factors that influence the hysteretic behavior of a certain steel bridge pier include all the constitutional parameters and axial load ratio P/P_y. The quantity P/P_y is determined in elastic seismic design and depends on the safety factor ν adopted in the preliminary design. Presently in practical design of thin-walled steel bridge piers, the safety factor is often made higher than the code-specified value (i.e. 1.14), thus variation of the safety factor ν should be taken into account in providing inelastic response spectra.

With reliable modeling of hysteretic behavior, inelastic response spectra can be generated based on Eq.(19). Computed displacement responses from Eq.(19) are further transformed into the spectral values $|\delta_{max}|/\delta_{95}$ (δ_{max} — maximum displacement response) and $|\delta_R|/h$. Since these two spectra values relate estimated demand to structural capacity, whether a preliminary design meets the code requirements can directly be read from the spectra. Counting influencing factors, the spectral values S ($|\delta_{max}|/\delta_{95}$ or $|\delta_R|/h$) should be in the form:

$$S = S\left(\textit{cross section shape},\ \bar{\lambda},\ \nu, T\right) \tag{20}$$

It is found that given the cross section shape and safety factor ν, the slenderness ratio parameter $\bar{\lambda}$ and the natural period T are correlated in elastic seismic design (T becomes longer with a larger value of $\bar{\lambda}$). Therefore, the inelastic response spectra can be specified in terms of three major factors as expressed by:

$$S = S\left(\textit{cross section shape},\ \nu, T\right) \tag{21}$$

The JRA code[1)] prescribes three Level 2 · Type I accelerograms and three Level 2 · Type II accelerograms under each ground type (Ground Type I, II and III) for dynamic analysis at ultimate limit state design stage, and suggests the average responses under three accelerograms (of the same Type , Type I or Type II) be taken as the final analysis results. In the inelastic response spectra presented in the next two sections, both $|\delta_{max}|/\delta_{95}$ and $|\delta_R|/h$ are actually the average of calculated responses under three different ground motions.

Analysis procedure for generating the inelastic spectra using the damage-based hysteretic model is summarized in the following:

1) Define the cross section shape and designate the kind of steel. In this step, structural parameters R_f (or R_t), also $\bar{\lambda}_s$ and $\bar{\alpha}$ (if it is a stiffened box section) can be determined.
2) Designate safety factor ν.
3) Designate slenderness ratio parameter $\bar{\lambda}$ (or pier height h).
4) Compute axial load P in elastic seismic design; (then axial force ratio P/P_y and system mass M can be determined)
5) Calculate natural period T.
6) Calculate parameters of the damage based hysteretic model.
7) Input design accelerograms and carry out time history analysis with Eq.(19).
8) Compute spectra values $|\delta_{max}|/\delta_{95}$ and $|\delta_R|/h$ (δ_{95} shall first be calculated from Eq.(17) or Eq.(18) depending on the cross section type).
9) Return to Step 3) and change $\bar{\lambda}$, the calculation will move to a different natural period. Repeat Step 3) to step 8) till the targeted range of T (or $\bar{\lambda}$) is fully covered.
10) Return to Step 2) and change safety factor ν, the calculation will move to a new spectrum. Repeat Step 2) to 9) till the targeted range of ν is covered.

5. Inelastic Response Spectra for Pipe-section Steel Bridge Piers

Suppose the kind of steel to be used is determined, a circular pipe section can be defined by the radius-thickness ratio parameter R_t and wall-thickness t. In this section, inelastic response spectra for three cross sections with different R_t values are plotted using the damage-based hysteretic model. The three cross sections are defined as follows:

1) R_t =0.100, t =20mm (Steel: SM490)
2) R_t =0.065, t =23mm (Steel: SM490)
3) R_t =0.050, t =23mm (Steel: SM490)

And model parameters of the damage-based hysteretic model are calculated by Eqs.(4)~(9).

The complete set of spectra for the above cross sections can be found in Ref. 5, here due to space limit, only the spectra of Ground Type II are shown in **Figs. 3~4** . Note that five discrete values between 1.14 and 2.0 are designated of the safety factor ν in the preliminary design, and ν =1.14 is the standard value suggested by the JRA code[1)]. It can be seen from these spectra that Type II accelerograms will generally cause far more severe inelastic deformations than Type I accelerograms. The fact that almost no crossed lines exist in the maximum response spectra indicates that heightening the safety factor will definitely reduce the maximum displacement response. However, the trend in residual displacement response is much more complicated: a higher safety factor in the elastic seismic design does not necessarily reduce the residual displacement to an acceptable level, especially under Type II accelerograms. And the residual displacement seems to be significantly affected by natural period. Comparing the spectra based on the three different cross sections, it can be seen that increasing the ductility capacity of the structure (adopting smaller radius-thickness ratio parameter R_t values) is an effective way to fulfill the code requirement on maximum displacement, but the level of residual displacement under Type II ground motions remains a major concern since decreasing R_t value from 0.100 to 0.050 seems to have little if any effect in bringing down the residual displacement

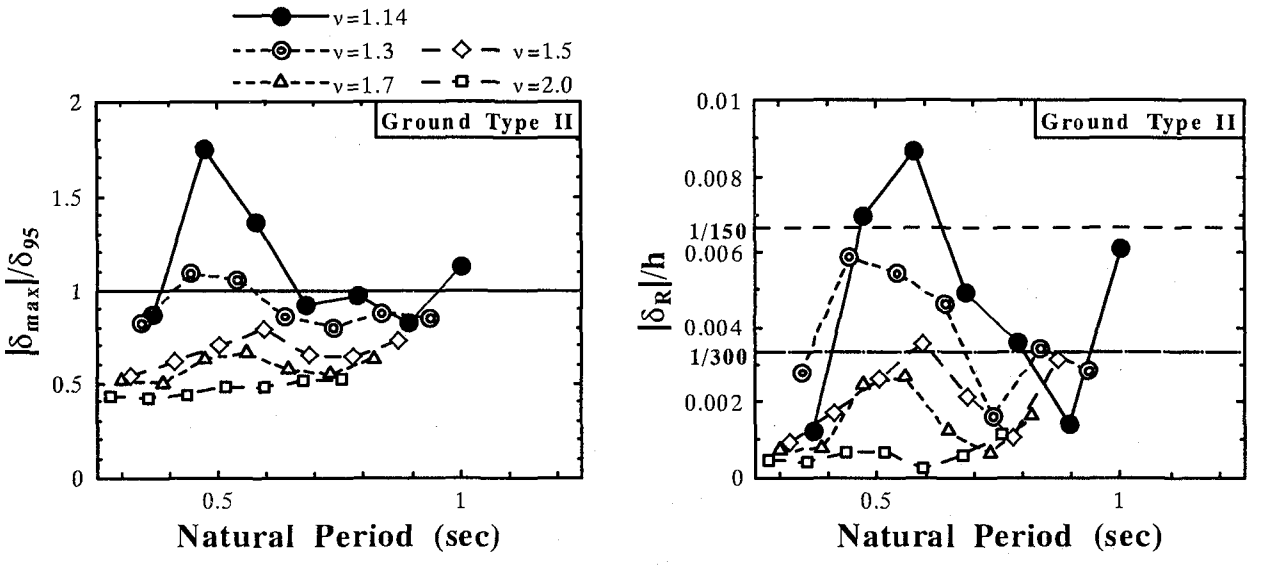

(a) cross section: $R_t = 0.10$, $t = 20mm$ (SM490)

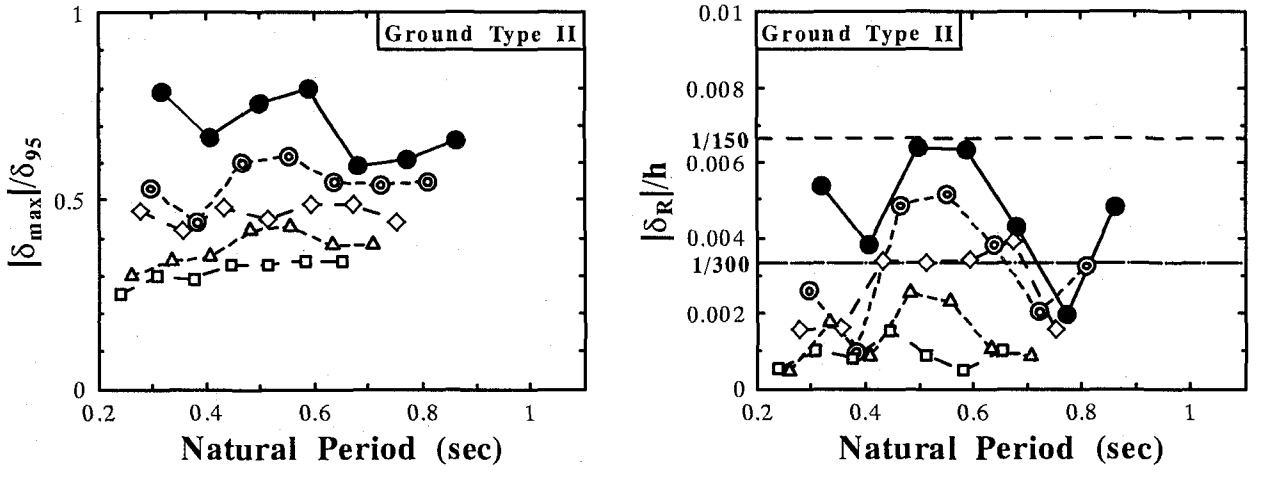

(b) cross section: $R_t = 0.065$, $t = 23mm$ (SM490)

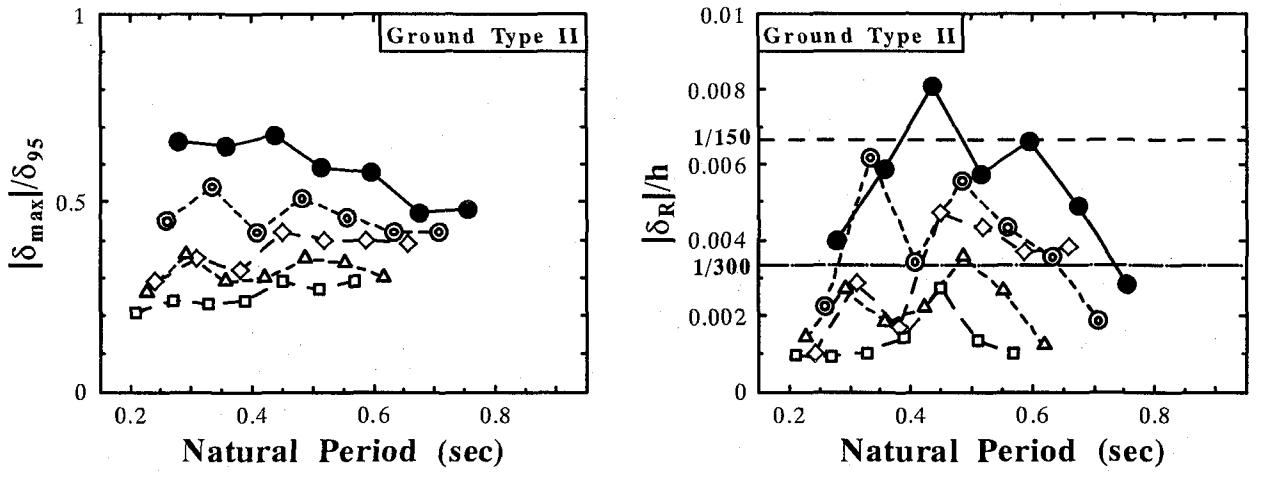

(c) cross section: $R_t = 0.050$, $t = 23mm$ (SM490)

Fig.3 Response spectra of pipe-section steel bridge piers under Level 2 · Type I accelerograms

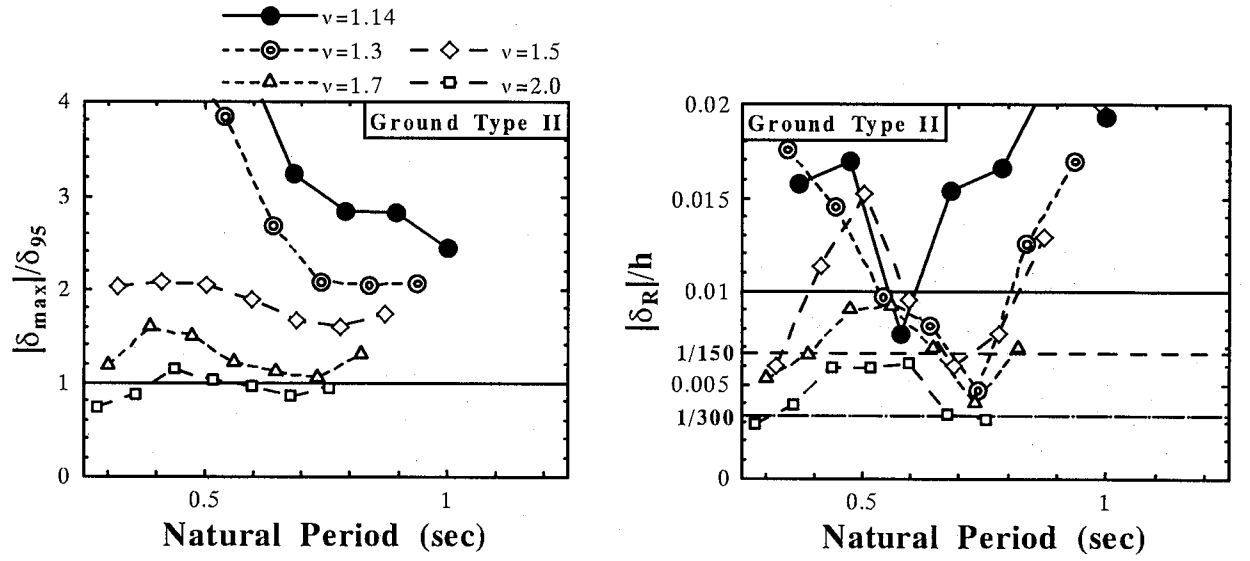

(a) cross section: $R_t = 0.10$, $t = 20mm$ (SM490)

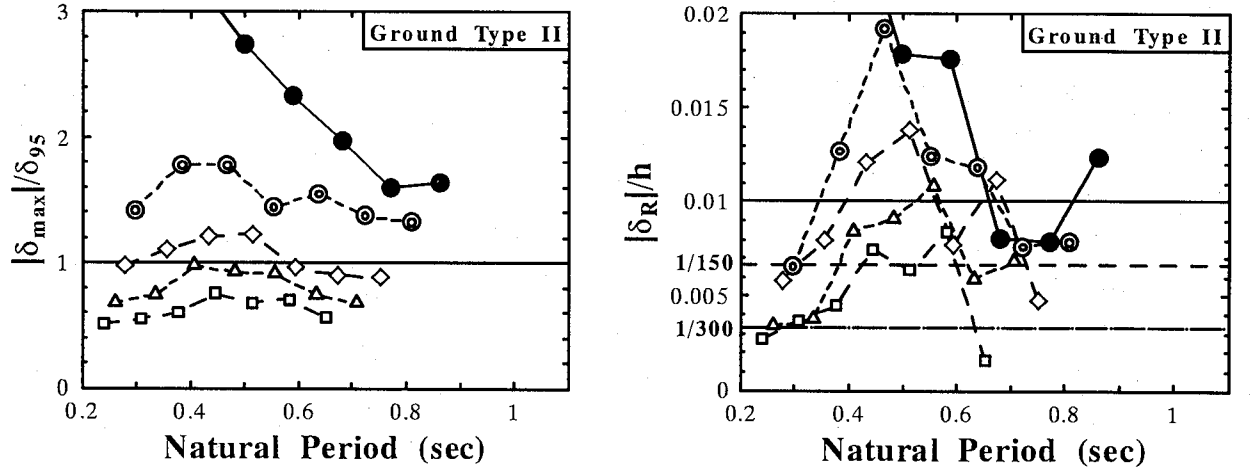

(b) cross section: $R_t = 0.065$, $t = 23mm$ (SM490)

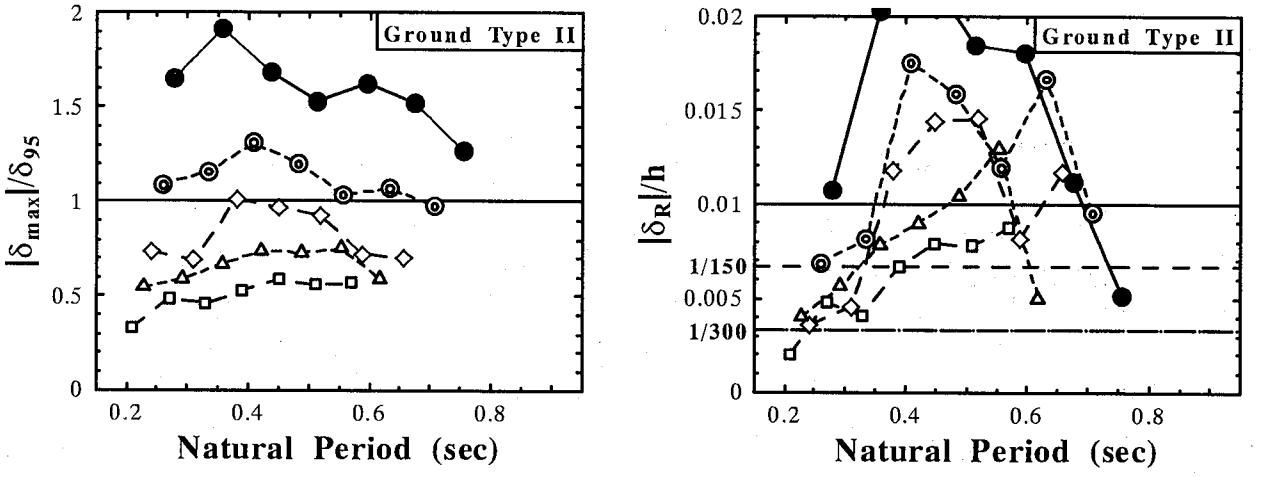

(c) cross section: $R_t = 0.050$, $t = 23mm$ (SM490)

Fig.4 Response spectra of pipe-section steel bridge piers under Level 2 · Type II accelerograms

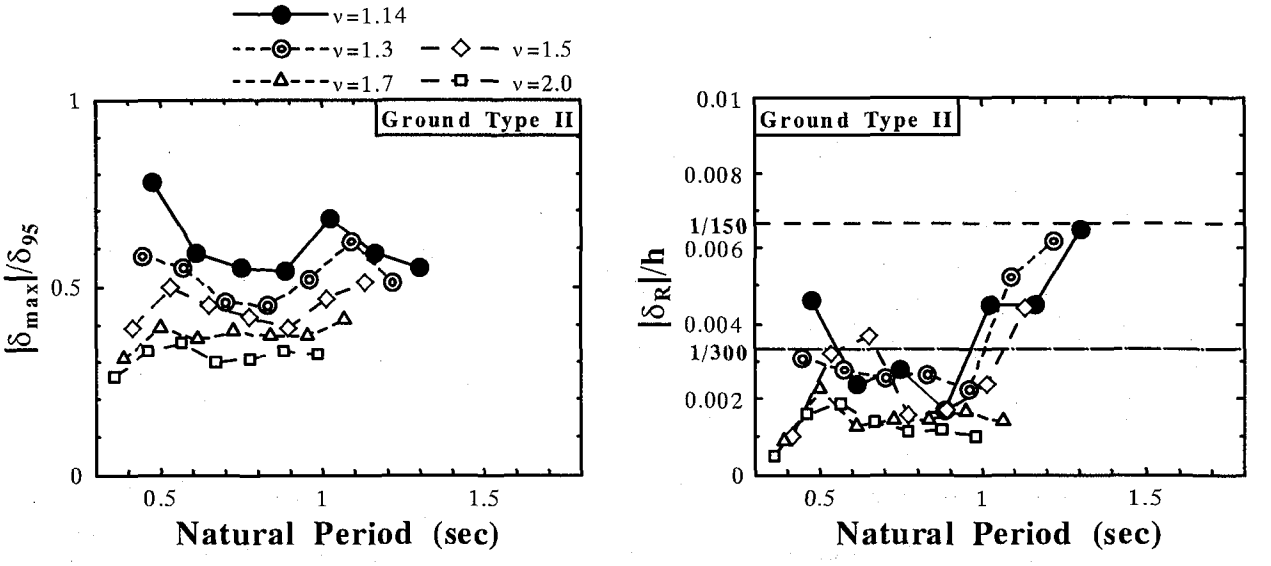

(a) cross section: $R_f = 0.45$, $t = 20mm$, $\gamma / \gamma^* = 3$, $\bar{\alpha} = 0.5$ (SM490)

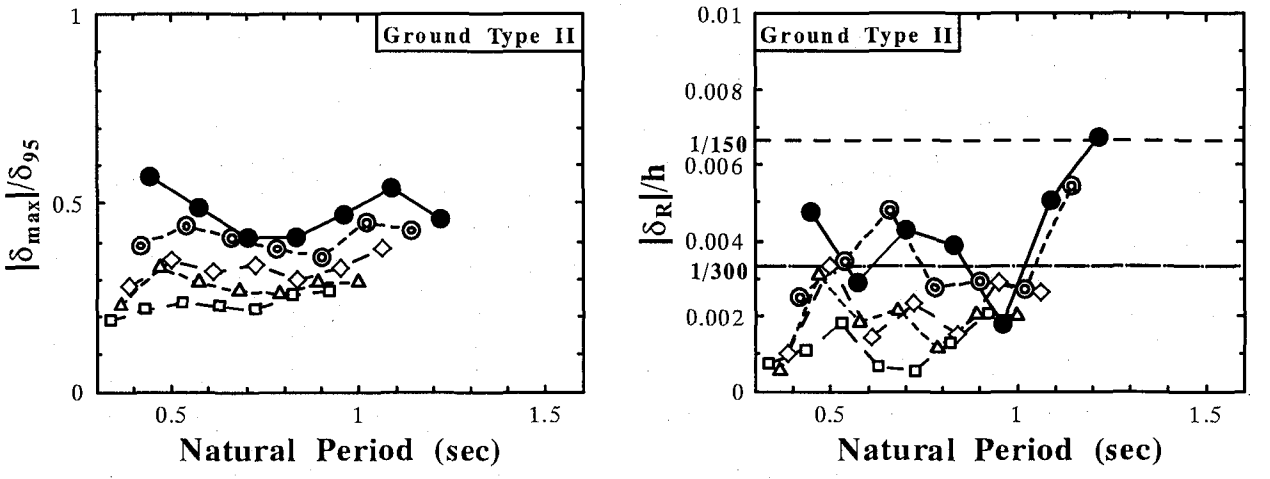

(b) cross section: $R_f = 0.35$, $t = 23mm$, $\gamma / \gamma^* = 3$, $\bar{\alpha} = 0.5$ (SM490)

Fig.5 Response spectra of box-section steel bridge piers under Level 2 • Type I accelerograms

level. It is also worth noting that the safety factor as suggested by the current JRA code[1] ν =1.14 generally turns out unsafe under Level 2 • Type II accelerograms as shown in the response spectra.

6. Inelastic Response Spectra for Stiffened Box-section Steel Bridge Piers

The inelastic response spectra presented in this section are based on the following two stiffened cross sections:

1) R_f =0.45, t =20mm, γ / γ^* =3, $\bar{\alpha}$ = 0.5 (Steel: SM490)
2) R_f =0.35, t =23mm, γ / γ^* =3, $\bar{\alpha}$ = 0.5 (Steel: SM490)

The major difference between cross section 1) and 2) is value of R_f.

Based on the damage-based hysteretic model (model parameters calculated according to Eqs.(10)-(15)), the spectra are plotted[5] and **Figs. 5~6** give the spectra of Ground Type II. It can be seen that with properly stiffened box-section steel bridge piers, adopting a safety factor of $\nu \geqq 1.5$ generally will limit both maximum displacement response and residual displacement to a repairable level. Under the code specified safety factor ν =1.14, estimated demand under Level 2 • Type II accelerograms comes within structural capacity only for a limited long-natural-period range (e.g. under Ground Type II conditions, the range is $T \geqq 1.24$ sec for the above cross section of R_f =0.45 and $T \geqq 0.96$ sec for the other cross section R_f =0.35).

7. Discussion on Inelastic Response Spectra for Pipe-section and Stiffened Box-section Steel Bridge Piers

From the inelastic response spectra presented in **Section 5** and **Section 6**, it seems that properly stiffened box-section steel bridge piers tend to have lower responses in terms of

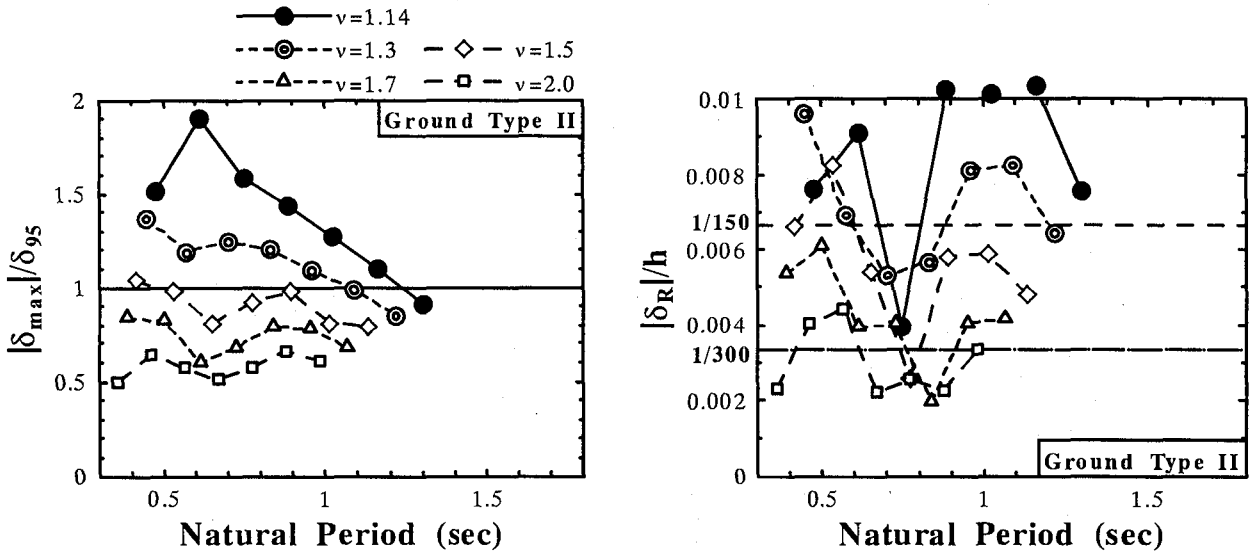

(a) cross section: $R_f = 0.45$, $t = 20mm$, $\gamma / \gamma^* = 3$, $\bar{\alpha} = 0.5$ (SM490)

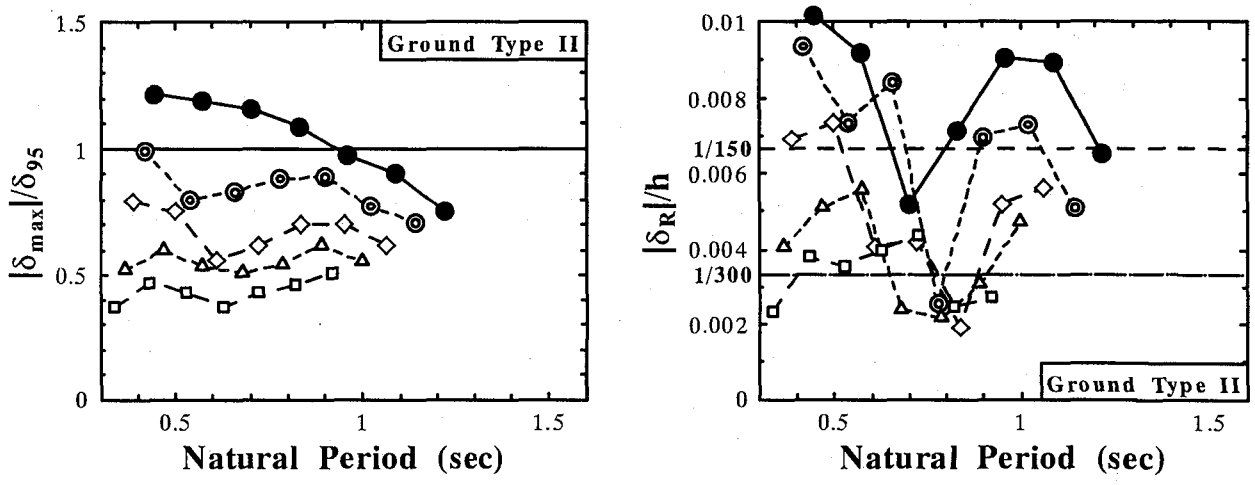

(b) cross section: $R_f = 0.35$, $t = 23mm$, $\gamma / \gamma^* = 3$, $\bar{\alpha} = 0.5$ (SM490)

Fig.6 Response spectra of box-section steel bridge piers under Level 2 • Type II accelerograms

demand versus capacity than pipe-section ones under a same safety factor value. In other words, properly stiffened box-section steel bridge piers tend to have larger safety margin in design. **Fig. 7(a)** is a comparison of cyclic ductility capacity δ_{95} / δ_y under the safety factor $\nu = 1.14$ between the pipe-section steel bridge piers of **Section 5** and the stiffened box-section steel bridge piers of **Section 6**. An interesting point in this graph is the good match of capacity (on a basis of equal $\bar{\lambda}$) between box-section piers with $R_f = 0.35$ and pipe-section piers with $R_t = 0.050$ as well as between the box-section piers with $R_f = 0.45$ and pipe-section piers with $R_t = 0.065$; In both pairs, capacities of box-section specimens are slightly lower, yet reflected in the inelastic response spectra is that box-section steel bridge piers generally have lower responses than their pipe-section counterparts.

The above phenomenon indicates that the safety margin for steel bridge piers to resist severe earthquakes is related not only to ductility capacities but also to cross section type. Understandably, cross section type shall have influence on both elastic stiffness and the magnitude of load from upper structure in elastic seismic design, thus it tends to affect also natural period of the structure. The difference in seismic responses can firstly be explained by the difference in natural period as illustrated in **Fig. 7(b)**. It can be seen that even with the same slenderness ratio parameter $\bar{\lambda}$, the analyzed stiffened box-section specimens have longer natural period than their pipe-section counterparts.

Since the dynamic analysis is based on the damage-based hysteretic model, it is worthwhile to do a little comparison between parameters of the damage-based hysteretic model for pipe-section specimens and those for stiffened box-section specimens. **Fig. 7(c)** and **Fig. 7(d)** are comparison of monotonic maximum strength $H_{max,1} / H_y$ and of monotonic ductility δ_u / δ_y respectively. It can be

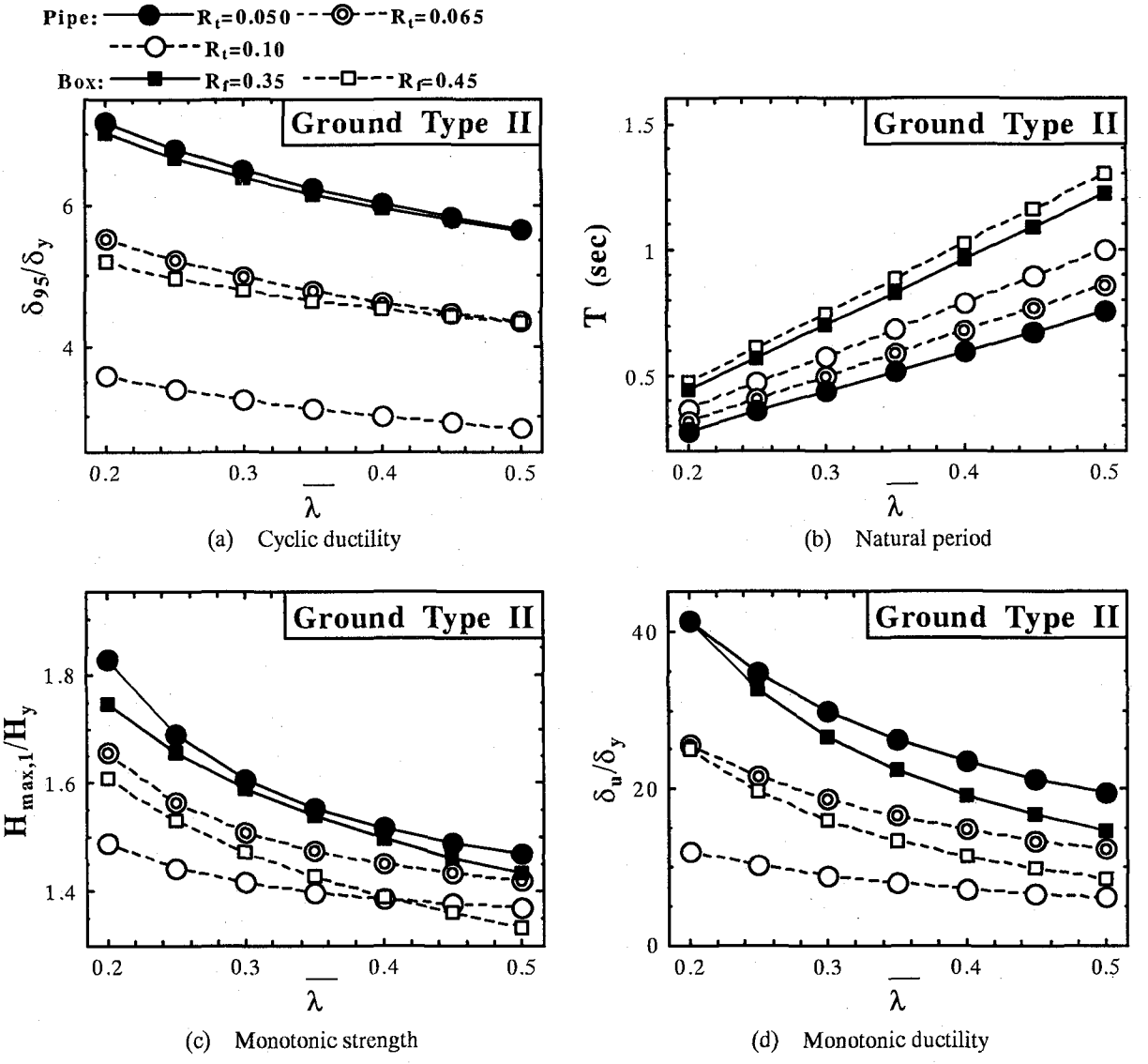

Fig.7 Inter-comparison among pipe-section and box-section steel bridge piers (preliminarily designed under $\nu = 1.14$)

seen that within the two pairs of similar δ_{95}/δ_y (between the box-section series of R_f =0.35 and pipe-section series of R_t =0.050 as well as between the box-section series of R_f =0.45 and pipe-section series of R_t =0.065), $H_{max,1}/H_y$ and δ_u/δ_y of the two pipe-section series seem to be superior to those of their box-section counterparts. Apparently, neither of these comparisons can account for the difference in dynamic responses.

Fig.8 compares the final damage index values (average results under three accelerograms) between the members of the two pairs. It can be seen that despite lower monotonic strength and monotonic ductility capacity of box-section specimens reflected in **Fig.7 (c)** and **Fig.7 (d)**, under both Type I and Type II accelerograms, the resulted damage in box-section specimens is definitely lower than that in their pipe-section counterparts, which explains the larger safety margin of box-section specimens. This trend in damage index may be attributed to the different free parameters β and c for pipe-section and stiffened box-section steel bridge piers. From the damage index expression (Eq.(1)), a larger parameter β gives more weight to hysteretic energy-based damage; It can be inferred that the influence of β on the final damage index values may depend on loading history. On the other hand, a larger parameter c will definitely result in a smaller damage index, and in turn slower strength and stiffness degradation in modeling hysteretic behavior. **Fig. 9** demonstrates the difference of c between stiffened box-section piers and pipe-section piers in the analysis: the values of c for stiffened box-section steel bridge piers are larger than those of pipe-section specimens when compared on a basis of equal $\bar{\lambda}$. To illustrate influence of β and c on the final damage index in dynamic analysis, a sensitivity study is carried out in which either β or c is designated an altered value (i.e. altered β for pipe-section specimens: 0.11, altered β for box-section specimens: 0.27; altered c for pipe-section

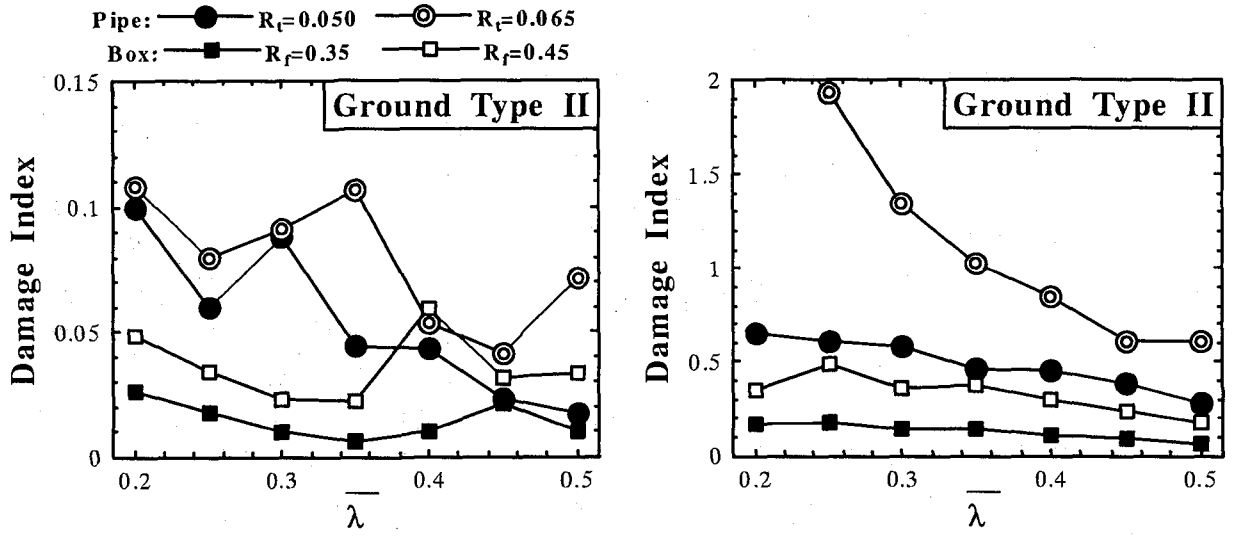

(a) Under Level 2 · Type I accelerograms (b) Under Level 2 · Type II accelerograms

Fig.8 Comparison of final damage index value between pipe and stiffened box specimens (preliminarily designed under $\nu = 1.14$)

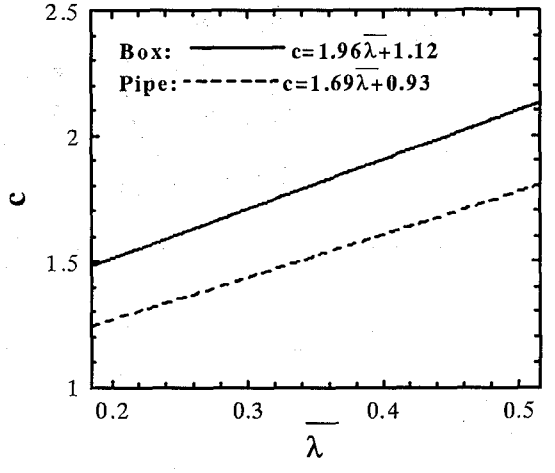

Fig. 9 Comparison of parameter c

specimens: $c = 1.96\bar{\lambda} + 1.12$; and altered c for box-section specimens: $c = 1.69\bar{\lambda} + 0.93$) for comparison with results under the rightful β or c values. **Fig.10** is comparison of damage index varying only β and **Fig.11** shows comparison of damage index varying only c. It can be seen that for both types of cross sections and under both Type I and Type II accelerograms, the larger parameter β tends to result in larger damage index, which indicates that hysteretic energy based damage is generally more significant than deformation-based damage under the Level 2 accelerograms. It can also be concluded from **Fig.10** and **Fig.11** that difference in parameter c between pipe and stiffened box steel bridge piers contributes much more to the difference in final damage index than difference in parameter β.

8. Summary and Conclusions

In the previous sections, the concept of inelastic response spectra under the Level 2 accelerograms for seismic design verification of steel bridge piers is introduced and some example spectra are plotted for a few typical pipe sections and stiffened box sections based on the damage-based hysteretic model. From these example spectra, it is found that:

1) Level 2 · Type II accelerograms will generally cause far more severe inelastic deformations than Level 2 · Type I accelerograms.
2) The code specified safety factor ν =1.14 for preliminary seismic design usually turns out unsafe for pipe-section steel bridge piers under Level 2 · Type II accelerograms. Properly stiffened box-section steel bridge piers preliminarily designed under ν =1.14 satisfy the ultimate limit state requirements only within a relatively long natural period range under Level 2 · Type II accelerograms.
3) A higher safety factor will definitely lower the maximum displacement response, but does not necessarily reduce residual displacement level.
4) Residual displacement response is significantly affected by natural period of the structure.
5) Increasing the ductility capacity of the structure (or reducing R_t or R_f value) is effective to fulfill code requirement on maximum displacement response, but is not equally effective in reducing residual displacement level.
6) The safety margin for steel bridge piers to resist severe earthquakes does not depend solely on structural capacity; It also has much to do with cross section type. Even with equal ductility capacity, properly stiffened box-section steel bridge piers tend to have larger safety margin than circular pipe-section steel bridge piers designed under the same conditions.

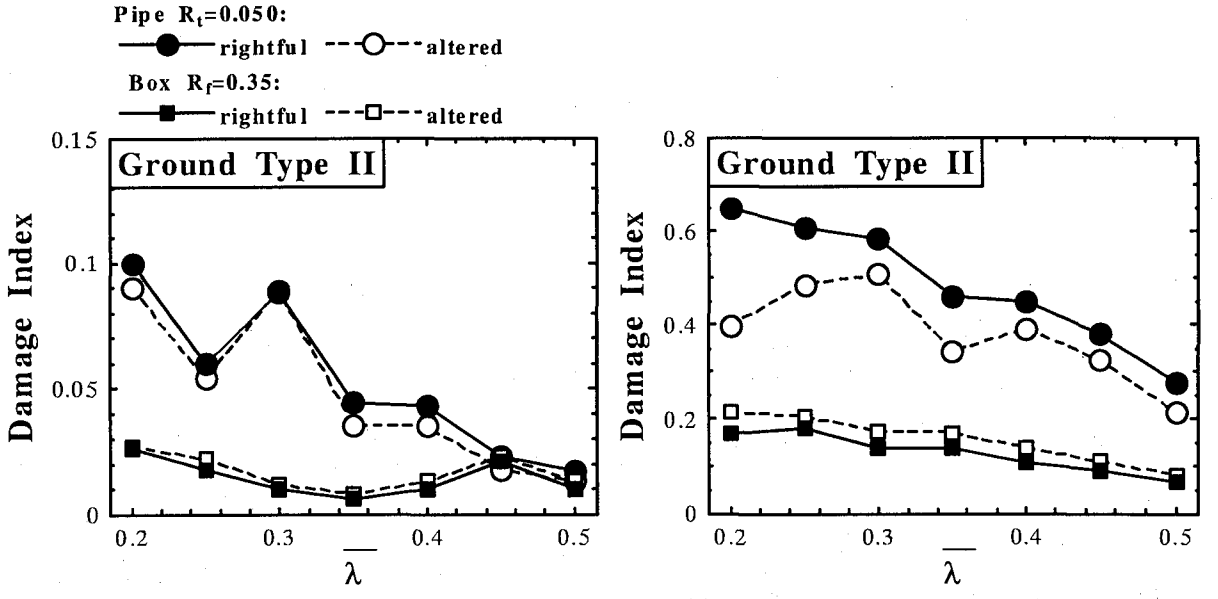

(a) Under Level 2 • Type I accelerograms (b) Underl Level 2 • Type II accelerograms

Fig.10 Comparison of final damage index varying only β

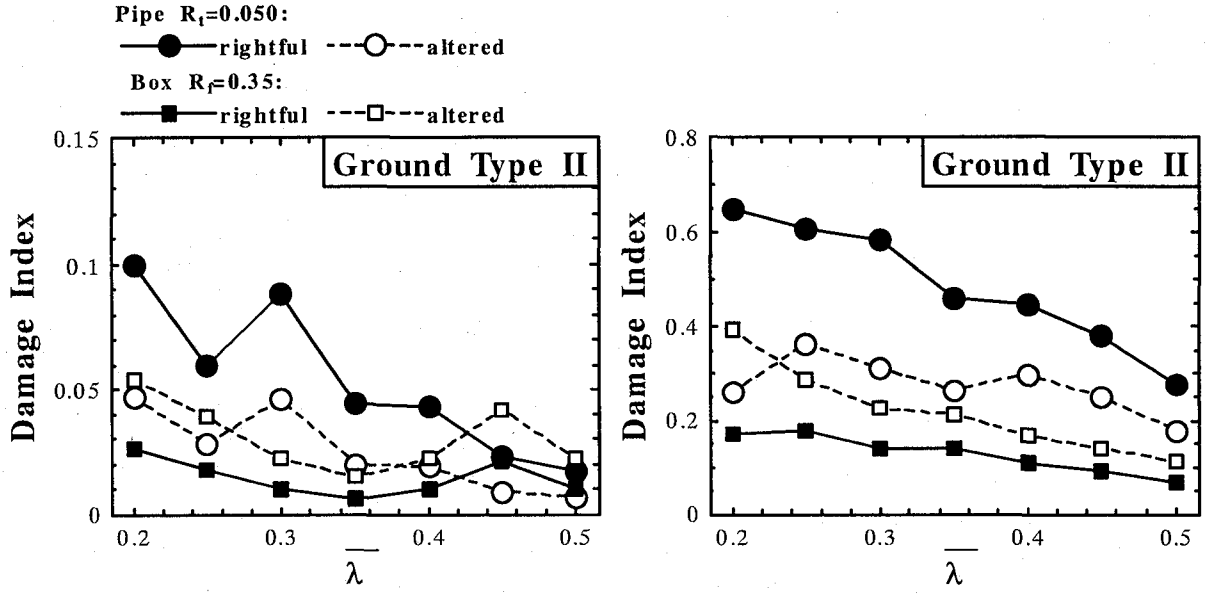

(a) Under Level 2 • Type I accelerograms (b) Underl Level 2 • Type II accelerograms

Fig.11 Comparison of final damage index varying only c

7) From the point of view of damage evaluation, the larger safety margin of stiffened box-section steel bridge piers is due to a larger parameter c and a smaller parameter β for properly stiffened box-section steel bridge piers than pipe-section steel bridge piers, which tend to result in a smaller damage index under the Level 2 accelerograms and in turn slower strength and stiffness degradation in modeling hysteretic behavior.

8) The comparisons of responses and capacities of pipe-section and stiffened box-section steel bridge piers in this study suggests that properly stiffened cross sections help reduce seismic demand.

With inelastic response spectra, seismic design verification of steel bridge piers can be done without time history analysis. Since the proposed spectra provide the whole picture of the trend in demand versus structural capacity, making full use of them can greatly reduce the number of repetitions needed in modifying a preliminary design. The spectra can even serve as an aid in selecting cross-section shape at the beginning of the whole design procedure. In short, inelastic response spectra will enable much more efficient seismic design of steel bridge piers.

Appendix I : Basic Structural Parameters of Steel Bridge Piers

1) Radius-thickness ratio parameter R_t for pipe-section steel bridge piers:

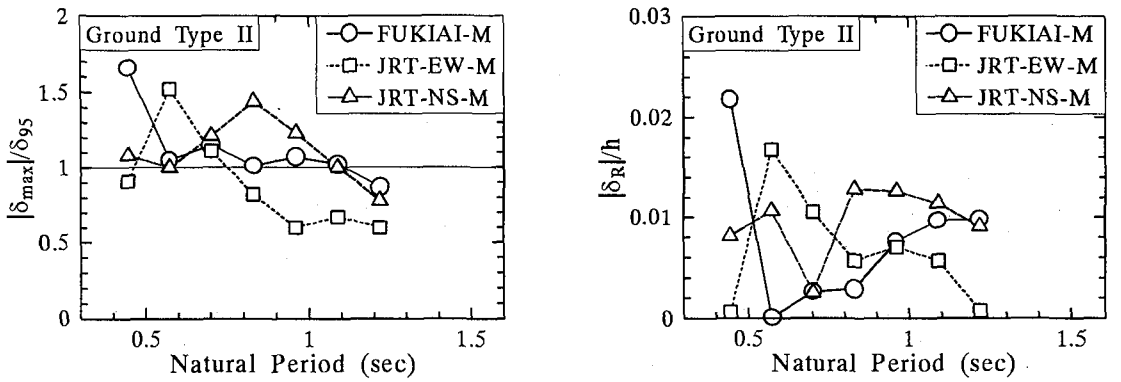

Fig.A1 The response spectra

R_t for pipe-section steel bridge piers is defined as[8]:

$$R_t = \sqrt{3(1-\nu^2)}\frac{\sigma_y}{E}\frac{D}{2t} \tag{A1}$$

wherein σ_y = yield stress of steel; E = Young's modulus; ν = Poisson's ratio; D and t = diameter and thickness of the cross section respectively.

2) Slenderness ratio parameter $\bar{\lambda}$

Slenderness ratio parameter $\bar{\lambda}$ for steel bridge piers (either box-section or pipe-section) is defined as[8]:

$$\bar{\lambda} = \frac{2h}{r}\frac{1}{\pi}\sqrt{\frac{\sigma_y}{E}} \tag{A2}$$

wherein h =column height and r = radius of gyration of the cross section.

3) Width-thickness ratio parameter of flange plate R_f for box-section steel bridge piers:

R_f for stiffened box-section steel bridge piers is defined as[8] :

$$R_f = \frac{b}{t}\sqrt{\frac{\sigma_y}{E}\frac{12(1-\nu^2)}{\pi^2 k}} \tag{A3}$$

wherein σ_y = yield stress of steel; E = Young's modulus; ν = Poisson's ratio; k = buckling coefficient of the flange plate, $k = 4n^2$ in which n = number of sub-panels divided by longitudinal stiffeners; b = width of the flange plate; t = thickness of the flange plate.

4) Equivalent slenderness ratio parameter of longitudinal stiffeners $\bar{\lambda}_s$ (box-section steel bridge piers)

Equivalent slenderness ratio parameter $\bar{\lambda}_s$ of longitudinal stiffeners is defined as[7]:

$$\bar{\lambda}_s = \frac{1}{\sqrt{Q}}\frac{L_d}{r_s}\frac{1}{\pi}\sqrt{\frac{\sigma_y}{E}} \tag{A4}$$

$$Q = \frac{1}{2R_f}\left[\bar{\beta} - \sqrt{\bar{\beta}^2 - 4R_f}\right] \tag{A5}$$

$$\bar{\beta} = 1.33R_f + 0.868 \tag{A6}$$

wherein L_d = distance between two diaphragms; r_s = radius of gyration of the T-shaped cross section centered on one longitudinal stiffener with a flange plate width of b/n.

Appendix II Difference of inelastic spectra under different accelerograms

In this paper, the inelastic response spectra are plotted from the average analysis results of three different design accelerograms of the same group according to the JRA code[1]. This specification is intended to consider the randomness of earthquake ground motion. For reference purpose, an example is given here to illustrate the difference of analysis results under different design accelerograms: The response spectra of box cross section steel bridge piers —$R_f = 0.35$, $t = 23mm$, $\gamma/\gamma^* = 3$, $\bar{\alpha} = 0.5$ (SM490) under the three Level 2-Type II (Ground Type II) design accelerograms are plotted in **Fig.A1** .

References

1) Design Specifications of Highway Bridges (Part V. Seismic Design), Japan Road Association, December 1996 (In Japanese).
2) S. Kumar and T. Usami: An evolutionary-degrading hysteretic model for thin-walled steel structures, *Engineering Structures,* Vol. 18, No.7, pp.504-514, 1996.
3) Q.Y. Liu, A. Kasai and T. Usami: Parameter identification of damage-based hysteretic model for pipe-section steel bridge piers, *Journal of Structural Engineering, JSCE,* Vol. 45A, pp.1005-1016, March, 1999.
4) T. Kindaichi, T. Usami and S. Kumar: A Hysteresis model based on damage index for steel bridge piers, *Journal of Structural Engineering, JSCE,* Vol. 44A, pp.667-678, March, 1998 (In Japanese)
5) Q.Y. Liu, A. Kasai and T. Usami: Inelastic Seismic Design Verification of Thin-walled Steel Bridge Piers, NUCE Research Report No. 9903, Dept. of Civil Engineering, Nagoya University, 1999.
6) S. B. Gao, T. Usami and H. B. Ge: Numerical Study on Seismic Performance Evaluation of Steel Structures, NUCE Research Report No. 9801, Dept. of Civil Engineering, Nagoya University, 1998.
7) Interim Guideline and New Technology for Seismic Design of Steel Highway Bridges, Committee on New Technology for Steel Structures, JSCE, July, 1996 (In Japanese).
8) Design Code For Steel Structures — Part A: Steel Structures In General, Subcommittee on Design Code For Steel Structures, Committee on Steel Structures, JSCE, 1987 (In Japanese).

(Received September 17, 1999)